Ultrafast Quenching of the Xanthone Triplet by Energy Transfer: New Insight into the Intersystem Crossing Kinetics

H. Satzger,[†] B. Schmidt,[†] C. Root,[†] W. Zinth,[†] B. Fierz,[‡] F. Krieger,[‡] T. Kiefhaber,[‡] and P. Gilch*,[†]

Department für Physik, Ludwig-Maximilians-Universität, Oettingenstrasse 67, D-80538 München, Germany, and Division of Biophysical Chemistry, Biozentrum, University of Basel, Klingelbergstrasse 50/70, CH-4056 Basel, Switzerland

Received: June 4, 2004; In Final Form: August 11, 2004

The formation and quenching of the triplet state of xanthone are studied by femtosecond techniques. As revealed by femtosecond fluorescence spectroscopy, the primarily excited $^1\pi\pi^*$ state decays within 1.5 ps. In a transient absorption experiment, this time constant is associated with a partial rise of a triplet signature. This rise has a second and slower component with a time constant of 12 ps. In the presence of high concentrations of the quencher 1-methylnaphthalene, the slow 12 ps rise component is absent. This finding gives strong evidence that the biphasic rise of the triplet absorption of xanthone is due to a sequential mechanism, namely, a $^1\pi\pi^* \rightarrow {}^3n\pi^*$ with fast intersystem crossing followed by a $^3n\pi^* \rightarrow {}^3\pi\pi^*$ internal conversion. Furthermore, an analysis of the concentration dependence of the quenching kinetics allows one to pin down the intrinsic transfer time of the triplet energy from xanthone to 1-methylnaphthalene to ∼1 ps.

1. Introduction

Many biological polymers have to form specific intramolecular interactions to be able to fulfill their biological function. The rate at which polymers can explore conformational space is limited by intrachain diffusion, that is, by the rate at which two points on a polymer chain can make contact. Experimental methods are therefore needed which allow direct measurement of intrachain diffusion rates. Triplet−triplet energy transfer (TTET) between a triplet donor (D) and a triplet acceptor (A) has recently been applied to measure intrachain contact formation in polypeptide chains to gain information on the dynamics of the earliest steps in the protein folding process.[1−3] In these experiments (see Figure 1), the two positions of interest on the polypeptide chain are labeled with a D/A pair. The donor is photoexcited, which marks the beginning of the detection period. When the donor meets the acceptor, an energy transfer process takes place transferring the triplet state to the acceptor. The transfer is detected by the concomitant absorbance changes. An ideal D/A system for such studies should have the following properties (see Figure 1): (i) The rate constant for formation of the excited donor state should be higher than the rate constant for intrachain diffusion ($k_{ex} \gg k_c$). (ii) The excited donor state should be very long-lived, so that the peptide dynamics can be traced throughout a large time window. (iii) The transfer rate constant between D and A should be higher than the rate constant for breaking of the contact ($k_{TT} \gg k_{-c}$), and (iv) the transfer rate should decay very rapidly with distance. A D/A system that matches these criteria is the couple xanthone (D) and naphthalene (A). Following photoexcitation, xanthone undergoes intersystem crossing (ISC) with a quantum yield close to 1[4] preparing a long-lived triplet state ($\tau = 20\ \mu$s in water[2]). The energy of this state can be transferred to the naphthalene. TTET occurs via a two-electron exchange process (Dexter mechanism); thus the transfer rate decays very rapidly with distance (and the transfer is only efficient for a close contact situation (van der Waals contact)).[5] By incorporation of xanthone and naphthalene moieties in a peptide chain, intramolecular contact time constants on the nanosecond time scale could be determined.[2,3] In these experiments, the donor triplet states were produced by a 4 ns laser flash and dynamics with time constants between 5 ns and several microseconds were observed, depending on the length and the sequence of the polypeptide chains.[2,3] Tests for the presence of faster chain dynamics on the subnanosecond time scale require a characterization of the photodynamics of the xanthone/naphthalene TTET pair in detail. This yields information on the limitations of the method in the early time region set by triplet formation and TTET dynamics.

The first transient absorption experiments on xanthone with picosecond resolution[6,7] yielded time constants for triplet formation in the 10 ps range. Later experiments with higher time resolution[8] revealed a biphasic rise of the triplet absorption $A(t)$; that is, the rise could be described by

$$A(t) = A_1(1 - \exp(-t/\tau_1)) + A_2(1 - \exp(-t/\tau_2)) \quad (1)$$

with time constants $\tau_1 \approx 1$ ps and $\tau_2 \approx 10$ ps and amplitudes A_1 and A_2. This biphasic behavior was attributed to a branched reaction scheme. In the proposed model (Figure 2a), the primarily excited $^1\pi\pi^*$ decays via two channels: internal conversion (IC) to the $^1n\pi^*$ state *and* ISC to the $^3n\pi^*$ state. The time constants of both processes were assumed to be similar. They should lead to the observed value of $\tau_1 \approx 1$ ps. Subsequently the $^1n\pi^*$ state is depleted by a second ISC process to the $^3\pi\pi^*$ state. This model obeys the El-Sayed rules for ISC processes:[9] For an ISC process for which the type of the orbitals occupied is changed (e.g., $n\pi^* \rightarrow \pi\pi^*$) in the course of the spin flip, a high ISC rate is expected. By this simultaneous change of spin and orbital character of the electronic wave

* To whom correspondence should be addressed. Fax: +49-89/2180-9202. E-mail: Peter.Gilch@physik.uni-muenchen.de.
[†] Ludwig-Maximilians-Universität.
[‡] University of Basel.

10.1021/jp047583+ CCC: $27.50
Published on Web 10/16/2004

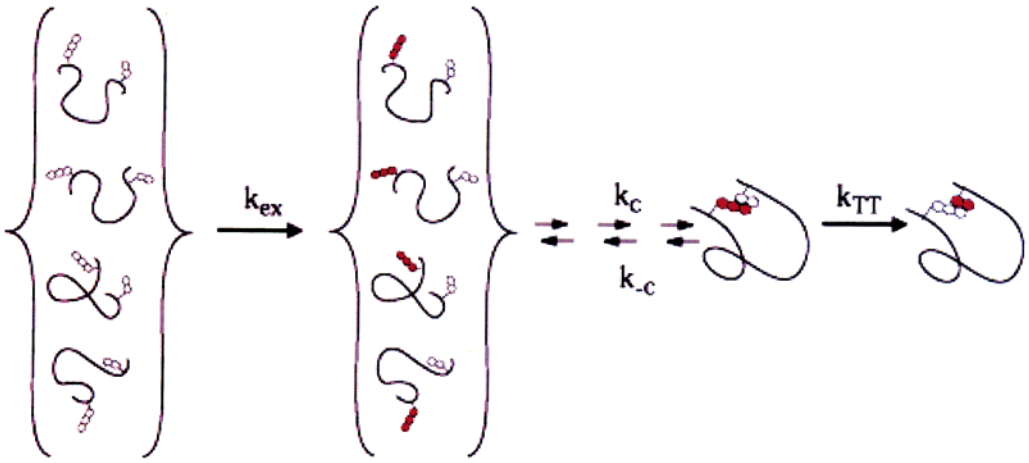

Figure 1. Principle of the experimental determination of contact rates in peptides. Two residues of a peptide chain are marked with an acceptor (A) and a donor (D), respectively. In a thermal ensemble of those marked peptides, the acceptor is photoexcited by a laser pulse. If during their diffusive motion the markers come into close contact, energy will be transferred indicating this contact.

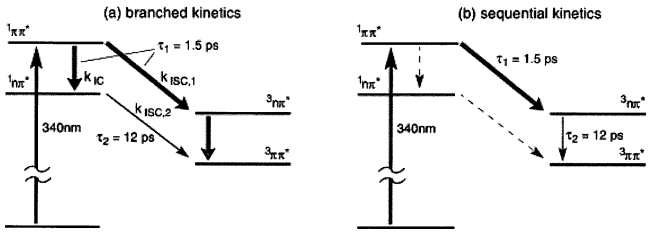

Figure 2. Jablonski diagram depicting the various excited states of xanthone and their potential decay patterns. (a) Branched kinetics. (b) Sequential kinetics. Rate constants for intersystem crossing processes are $k_{ISC,1,2}$, and those for internal conversion are $k_{IC,1,2}$. Only ISC processes allowed by the El-Sayed rules are considered. Thick arrows represent large rate constants.

function, the change of the spin angular momentum in the ISC can be compensated by a corresponding change of the orbital angular momentum. Obviously, the branched kinetic scheme proposed in ref 8 is in agreement with these rules. However, an alternative model with sequential kinetics (Figure 2b), that is, fast ISC from the $^1\pi\pi^*$ to the $^3n\pi^*$ state followed by slower internal conversion in the triplet manifold to the $^3\pi\pi^*$, cannot be ruled out. The authors of ref 8 assumed that only the final product state in the sequential process is spectroscopically visible at the single detection wavelength used in ref 8. Under this assumption, a sequential process would lead to amplitudes A_1 and A_2 with opposite sign. The observation of the same signs of A_1 and A_2 pointed to branched kinetics. However, if the intermediate state contributes to the observed time trace its extinction coefficient has to be taken into consideration and a decision between branched and sequential kinetics with the present information is not possible.

In this paper, we will readdress the ISC of xanthone and we will have a close look at the quenching of the xanthone triplet by naphthalene. We will deal with the problem by combining three experimental approaches. (i) The decay of the fluorescence of xanthone, that is, the depletion of its primarily excited state, is monitored using an ultrafast Kerr shutter. (ii) The formation of the triplet state of xanthone is followed by spectrally resolved transient absorption spectroscopy in a broad spectral range. (iii) Finally, the influence of a quencher, 1-methyl-naphthalene, on the absorption dynamics is investigated. These experiments not only aim at the dynamics of the quenching itself but will yield a deeper insight into the mechanism of the ISC of xanthone, a prerequisite for using this D/A pair as a sensor for the investigation of peptide closure dynamics in the picosecond realm.

2. Experimental Section

The setup for femtosecond fluorescence experiments has been described before in detail in ref 10. Briefly, a Clark CPA 2001 laser/amplifier system (repetition rate of 1 kHz) pumped a two-stage noncollinear optical parametric amplifier (NOPA) tuned to 540 nm. The compressed output of the NOPA was frequency doubled in a 100 μm type I BBO crystal. The resulting 270 nm pulses with an energy of 0.2 μJ are used to excite the xanthone sample. The fluorescence light emitted by the sample is imaged onto a Kerr gate consisting of two wire grid polarizers and a fused silica plate. The Kerr gate is operated by femtosecond NIR (1100 nm) laser pulses obtained from a two-stage optical parametric amplifier (OPA) again pumped by the laser/amplifier system. The fluorescence light that passed the Kerr gate was dispersed by a spectrometer and detected by a liquid nitrogen cooled CCD camera. Parasitic stray light was suppressed by a UG 5 filter (to reject the NOPA fundamental at 540 nm) and KG 5 (to reject the ~1100 nm gate light). The time resolution of the setup in the near UV was ~200 fs (full width at half-maximum (fwhm)). The xanthone fluorescence emission lies in the blue wing of the detection window of the Kerr setup where its spectral sensitivity starts to drop drastically. This circumstance requires prolonged acquisition times which cause an instrumental artifact. The irradiation of the Kerr medium by the gate pulses induces a very weak background gradually rising with time. The rising background signal feigns a long-lived emission of xanthone. Experimental runs with the excitation light blocked, that is, in the absence of the xanthone emission, allow that contribution to be estimated and the intrinsic behavior of xanthone to be extracted.

Femtosecond absorption spectra were recorded with the setup detailed in ref 11. As in the fluorescence experiments, the sample was excited by the frequency doubled output of a NOPA pumped by a conventional 1 kHz Ti:Sa laser/amplifier system. Two wavelengths were used for the excitation process: 266 and 340 nm. The excitation energy was equal to ~400 nJ at the sample location for both wavelengths. Absorption changes induced by these pump pulses were probed by a white light continuum generated by focusing a portion of the amplifier fundamental into a CaF_2 plate. The white light was split into a probe and reference branch. Both probe and reference continua were spectrally dispersed and recorded in single shot fashion

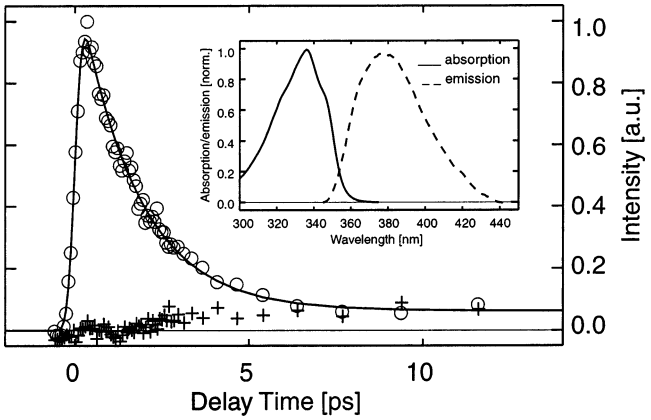

Figure 3. Decay of the fluorescence emission of xanthone at 414 nm (○) following 270 nm excitation recorded with a Kerr setup. The contribution of a slowly rising background emission is included (+). In this blank experiment, all parameters were identical to the experiment on the xanthone except for the blocked excitation light. The insert shows the absorption and fluorescence spectra of xanthone in ethanol.

by diode arrays.[12] The probe continuum overlaps in the sample with the pump light, and the reference continuum passes through a part of the sample not excited by the pump light. The pump−probe spectra were recorded with a magic angle setting.

For the femtosecond experiments, xanthone (Fluka) was dissolved in absolute ethanol (Merck, VLSI Selectipur). The concentrations of the sample solutions were in the range of 2−5 mM. The concentrations of 1-methylnaphthalene (Fluka) were adjusted by adding the respective volumes to the solutions. Xanthonic acid was synthesized and purified as decribed in ref 2. The concentrations of the acid in water and ethanol were about 0.5 mM. The solutions were exchanged between the laser shots by pumping them through fused silica flow cells (optical path length of 0.5 mm in the absorption experiment and 1 mm in the fluorescence experiment).

Transient absorption data in the nano- to microsecond realm were collected using a laser flash photolysis reaction analyzer (LKS.60) from Applied Photophysics. Xanthone was excited selectively by using a Quantel Nd:YAG laser (354.6 nm, 4 ns pulse of 50 mJ). For the pseudo-first-order quenching experiments, xanthone (Fluka, purum) was dissolved in ethanol (Merck, Uvasol) to a concentration of 0.05 mM measured by UV spectroscopy ($\epsilon_{335} = 6700\ M^{-1}\ cm^{-1}$). 1-Methylnaphthalene (Fluka, purum; $\epsilon_{280} = 6000\ M^{-1}\ cm^{-1}$) was added to concentrations ranging from 1 to 10 mM. The temperature was 295.6 K. The kinetics was typically measured five times, averaged, and analyzed using ProFit (Quansoft, Zürich, Switzerland). All rate constants were obtained by fitting the decay of the xanthone triplet at 610 nm.

Steady-state absorption and fluorescence spectra were recorded with a diode array spectrometer (Specord S100) and a Fluorolog 1680 0.22 m double spectrometer from Specs, respectively.

3. Results

3.1. Fluorescence Decay of Xanthone. When excited with UV light, xanthone emits a very weak fluorescence peaking around 380 nm (see the insert in Figure 3). A rough estimate for the lifetime of the excited $^1\pi\pi^*$ state may be obtained from the fluorescence quantum yield and the application of the Strickler−Berg relation[13] yielding a lifetime of the $^1\pi\pi^*$ state of the order of $\tau_1 = 1$ ps. Direct experimental access to τ_1 is obtained by measuring the time dependence of the emission decay with the help of a Kerr shutter setup. A typical time trace

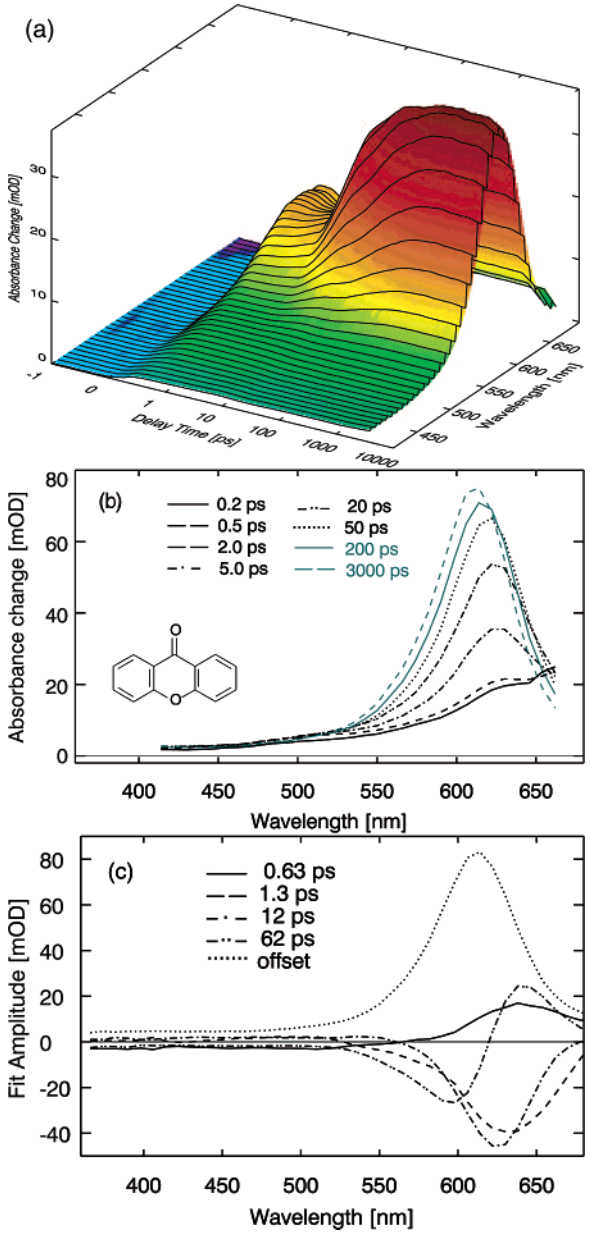

Figure 4. Transient absorption spectra of xanthone following 340 nm excitation. (a) Overview. (b) Transient spectra at distinct delay times. (c) Decay associated spectra.

is depicted in Figure 3. After an instrumentally limited rise, the fluorescence emission decays within ∼1 ps. The weak background observed stems from emission of the Kerr medium induced by the gate pulses. This weak emission gradually rises with time and is responsible for the small offset (see the time trace recorded with the excitation light blocked in Figure 3). Thus, only the initial emission decay originates from the xanthone sample. An exponential fit considering the experimental response function yields a time constant of ∼1.5 ps. Since the emission monitors the population of the excited $^1\pi\pi^*$ state, we can conclude that this state decays with $\tau_1 \sim 1.5$ ps. As this value is in line with the prediction based on fluorescence quantum yield, a contribution of a long-lived component, for which the Kerr setup is not very sensitive, can be ruled out.

3.2. Transient Absorption Spectroscopy. Absorption changes of xanthone with the femtosecond excitation tuned to the maximum of its $\pi\pi^*$ transition (340 nm) were recorded in a spectral region ranging from 370 to 700 nm (Figure 4a gives an overview of the data, and transient spectra at selected delay

times are depicted in Figure 4b). Immediately after photoexcitation, a weak and broad transient absorption peaking around 700 nm is formed (excited-state absorption from the $^1\pi\pi^*$ state). The decay of this signature within ~1 ps gives way to a stronger and sharper feature centered around 620 nm. The 620 nm band continues to rise during ~15 ps. On the time scale of our experiments (up to 3.5 ns), this feature remains constant in amplitude, though the center of the spectrum slightly shifts to the blue on the 50 ps time scale. To obtain quantitative information on the kinetics, the data were subject to a global fitting procedure. As a model function, a sum of exponentials (decaying absorption corresponds to positive amplitudes) convoluted with an instrumental response (Gaussian with a width of 200 fs fwhm) was used. A satisfactory agreement between data and fit was obtained using four exponentials and an offset to account for the triplet absorption persistent in the time range (up to ~3 ns) of the femtosecond experiment. The time constants derived are ~0.5, 1.3, 12, and 62 ps, and the corresponding decay associated spectra are depicted in Figure 4c. The spectra associated with the time constants of 1.3 and 12 ps both have negative sign (indicative for the buildup of an absorption) throughout most of the spectral region covered and are similar though not identical in shape. The 62 ps spectrum is sigmoidal, representing a blue shift of the ~620 nm band with time. The spectrum of the offset peaks at 610 nm and has a width of 50 nm (fwhm). From comparison of this spectrum with the spectrum obtained by nanosecond spectroscopy,[14] it can be safely assigned to the absorption of the relaxed triplet state of xanthone in ethanol. Transient absorption experiments have also been performed with the excitation tuned to 266 nm. The observed transient spectra and derived time constants are virtually identical to those in the experiments presented above (excitation wavelength of 340 nm). Thus, the different excitation wavelengths in the fluorescence and the absorption experiments do not seem to alter the photodynamics and the two may be directly compared. Very similar results were also obtained for xanthonic acid in ethanol (data not shown). Xanthonic acid in water shows similar kinetics in the time domain $\tau < 200$ ps. However, the blue shift of the triplet absorption band occurs here with a 300 ps time constant (data not shown).

3.3. Triplet Quenching by 1-Methyl-naphthalene (1-MN). Naphthalene and derivatives are known to quench the triplet states of aromatic ketones such as benzophenone and xanthone at least partially via intermolecular energy transfer.[15,16] The question of whether electron transfer can compete with energy transfer will be addressed below. In the following, the dependence of the photokinetics of xanthone on the concentration of the naphthalene derivative 1-MN is investigated. These experiments not only allow us to draw conclusions on the quenching dynamics but also help to elucidate the ISC mechanism of xanthone. Addition of 1-MN to a solution of xanthone reduces the lifetime of the triplet spectrum centered around 610 nm (see Figure 5). For low quencher concentrations of ≤0.01 M, the lifetime reduction can be traced by nanosecond laser flash photolysis. Here, the rate constant k_{TT} of the decay of the xanthone triplet absorption scales linearly with the quencher concentrations (Figure 7). Higher quencher concentrations require femtosecond techniques to time resolve the energy transfer dynamics. This is illustrated by a measurement performed on xanthone in the presence of 0.6 M (10 vol %) 1-MN (Figure 5). The 610 nm absorption with an "infinite" lifetime in pure ethanol now decays in ~100 ps. Synchronized with this decay, a spectrum centered around 420 nm rises. This spectrum can be safely assigned to the triplet state of 1-MN;[17,18] that is,

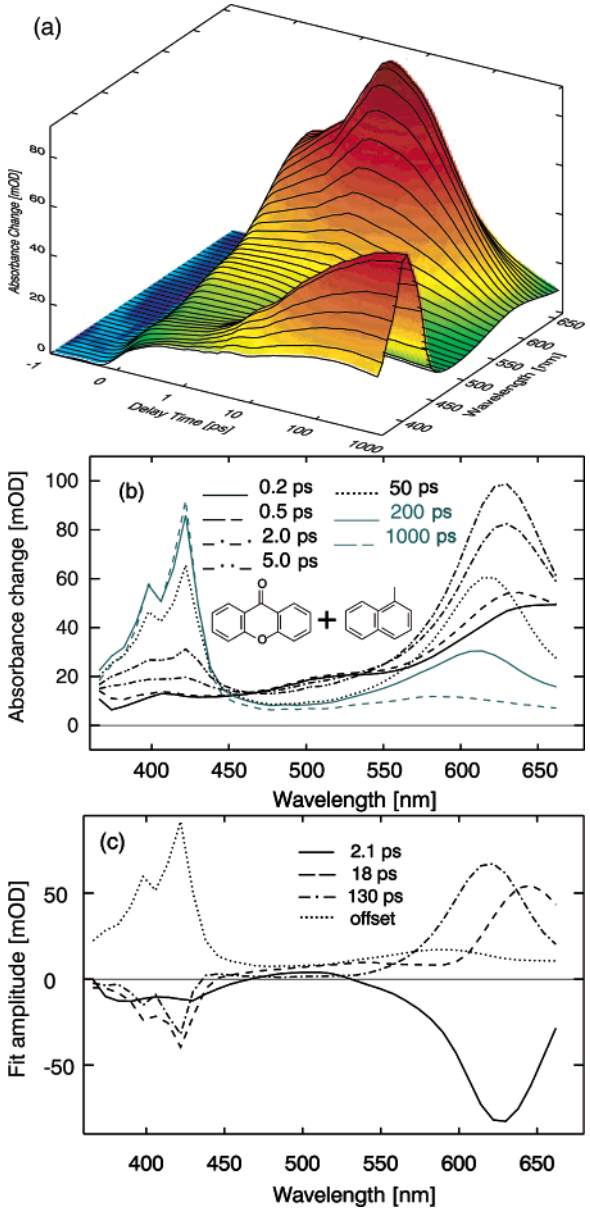

Figure 5. Transient absorption spectra of xanthone in the presence of 0.6 M 1-MN following 340 nm excitation. (a) Overview. (b) Transient spectra at distinct delay times. (c) Decay associated spectra.

as expected for an energy transfer process the decay of the xanthone triplet goes along with the population of the 1-MN triplet.

The temporal behavior of this transfer for various quencher concentrations can be nicely represented by two spectral integrals (Figure 6). The first integral (550−650 nm) covers the triplet absorption of xanthone (lower part of Figure 6), and the second integral (414−438 nm) that of the 1-MN. In the absence of a quencher, the biphasic rise of the xanthone triplet absorption is clearly represented by the "610 nm" integral. The "420 nm" integral is virtually "silent". In the presence of 0.06 M 1-MN, the kinetics of the rise is not altered but now the 610 nm integral decays with a time constant of ~1.5 ns. In parallel, the 420 nm integral rises with the same time constant. Increasing the 1-MN concentration by a factor of 10 has the expected effect of accelerating the decay of the 610 nm integral and the rise of the 410 nm integral by roughly the same factor. A closer inspection of that rise shows that it is multiphasic and its description with exponentials requires at least three terms with

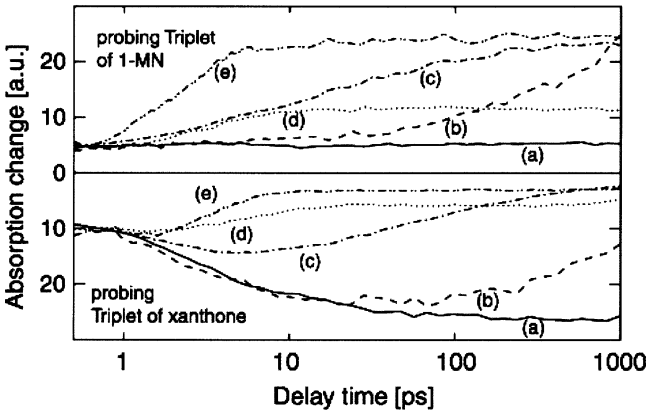

Figure 6. Time dependences of the spectral integrals covering the absorption of the 1-MN triplet (upper part) and that of the xanthone triplet absorption (lower part) for different 1-MN concentrations. For a better representation, the time traces in the lower part have been turned upside down. The 1-MN concentrations were (a) 0 M, (b) 0.06 M, (c) 0.6 M, (d) 3.0 M, and (e) neat 1-MN.

time constants of 2, 15, and 120 ps. The amplitudes of these terms are comparable. Note that the 2 ps time constant is shorter than the slow component observed for the rise of the xanthone triplet in the absence of a quencher. For the highest quencher concentration, that is, when performing the experiment in neat 1-MN, one obtains very fast and very simple quenching kinetics. The 420 nm integral rises in 2 ps, and the integral representing the xanthone triplet absorption decays in 2 ps to a small offset. Inspection of the spectrally resolved data (not shown) clearly demonstrates that this offset stems from a tail of the 1-MN triplet absorption and not from a residual xanthone triplet population.

Surprisingly, for a concentration of 3.0 M kinetics is found that deviates from the overall trend. In addition to the ultrafast kinetics which is comparable to the behavior in neat 1-MN, a longer lived component with a time constant of 1 ns appears that is absent even in the 0.6 M experiment. A possible origin for this anomaly will be addressed in the discussion.

4. Discussion

4.1. Intersystem Crossing in Xanthone. *Ultrafast Spectroscopy of Xanthone.* The time-resolved fluorescence data presented here allow us to exactly pin down the decay time of the primarily excited $^1\pi\pi^*$ state of xanthone. In previous time-resolved absorption experiments,[8] this time could only be inferred indirectly from the rise of the triplet spectrum. Among the four excited states ($^1\pi\pi^*$, $^3\pi\pi^*$, $^1n\pi^*$, and $^3n\pi^*$) within energetic reach of the photoexcitation, only the $^1\pi\pi^*$ state shares an appreciable transition moment with the ground state. Transitions from the singlet ground state to the two triplet state are spin forbidden, and the transition to the $^1n\pi^*$ state is forbidden by symmetry. The extinction coefficient for that transition is 6 M^{-1} cm^{-1} as compared to 12 000 M^{-1} cm^{-1} for the allowed transition to the $^1\pi\pi^*$ state.[19] Thus, the only emissive state is the $^1\pi\pi^*$ state and the decay of the fluorescence with a time constant of $\tau \sim 1.5$ ps[32] can be safely assigned to the depletion of this state. If the 1.5 ps time constant characterizes the depletion of the $^1\pi\pi^*$ state, the additional 0.5 ps component present in the transient absorption experiment has to be associated with relaxation processes within the $^1\pi\pi^*$ state and not with its decay.

From the three states that might be populated in the course of the $^1\pi\pi^*$ decay, the $^3\pi\pi^*$ state can be excluded since such a transition would violate El-Sayed's rules. Thus, only the $^1\pi\pi^* \rightarrow {}^1n\pi^*$ IC process (rate constant $k_{IC,1}$) and the $^1\pi\pi^* \rightarrow {}^3n\pi^*$ ISC process (rate constant $k_{ISC,1}$) have to be taken into consideration. The sum of the rate constants $k_{IC,1} + k_{ISC,1}$ is equal to the observed rate constant for the decay of the emissive state ($k_{IC,1} + k_{ISC,1} = 1/\tau_1 = (1.5\ \text{ps})^{-1}$). Partioning that decay into the two channels requires additional information on the involved states. The global analysis of the transient absorption spectra associates the rise of a strong absorption band around 610 nm with the $\tau_1 = 1.5$ ps kinetic component. The shape and position of that spectrum are very close to those of the triplet spectrum of xanthone reported in the literature.[4] Thus, it seems likely that the 1.5 ps process populates at least partially a triplet state. On the other hand, the singlet $^1n\pi^*$ state could have a very similar spectral signature to the $^3n\pi^*$ state and therefore a contribution or even a domination of the $^1\pi\pi^* \rightarrow {}^1n\pi^*$ IC process cannot be excluded on the basis of these results.

The next process (time constant of 12 ps) in the biphasic rise of the triplet absorption is characterized by a spectrum which is slightly blue shifted and has a somewhat smaller width than the 1.5 ps spectrum. This spectrum represents the changes associated with the population of the finally reached triplet state. The sigmoidal feature with a characteristic time of 62 ps observed thereafter describes a blue shift of the triplet absorption. A similar effect has been found for the thio-analogue of xanthone (thioxanthone).[20] By examination of this shift for thioxanthone in several solvents, it was demonstrated that the characteristic times of this shift correlate with the dielectric responses of the solvents.[20] For ethanol, a value of 72 ps was derived which nicely matches the value reported here. Thus, the 62 ps time constant is not associated with a buildup of the triplet absorption and the 12 ps kinetic component thus describes the slowest part of this rise. Special care has to be taken for the assignment of this ~12 ps kinetic component. The assignment of the observed absorption changes depends on the reaction model. They may result either from an increase of the population in the triplet manifold, that is, from the $^1n\pi^* \rightarrow {}^3\pi\pi^*$ transition (branched kinetics, Figure 2a), or from a $^3n\pi^* \rightarrow {}^3\pi\pi^*$ transition (sequential kinetics, Figure 2b). In the latter case, the absorption spectra of the two triplet states have to be similar in shape but the extinction coefficient of the $^3\pi\pi$ state has to be approximately twice that of the $^3n\pi^*$ state. Since no independent access to these extinction coefficients is available, a final decision between branched and sequential kinetics on the spectroscopic results alone is still not possible. Here, the quenching experiments come into play.

Quenching Kinetics: Dynamic and Static Limit. For bimolecular quenching experiments, two limiting cases are known: the dynamic and static regimes. For low concentrations of the quencher (dynamic regime), the kinetics is pseudo-first-order (even the lowest quencher concentration applied in this paper is much higher than the xanthone concentration) with the rate constant k_{TT} given[5] by

$$k_{TT} = k_q[\text{1-MN}] \qquad (2)$$

The plot of the quenching rate constant versus the 1-MN concentration (Figure 7) confirms this simple law for concentrations lower than 0.06 M. Note that this plot includes results obtained by nanosecond and femtosecond experiments. The bimolecular rate constant k_q obtained by a linear fit of the data in Figure 7 is 7.2×10^9 M^{-1} s^{-1} and is close to the value of 5.4×10^9 M^{-1} s^{-1} predicted by a simple Smoluchowski−Stokes−Einstein treatment.[21] This indicates that in this concentration regime the quenching is controlled by diffusion.

Simple single-exponential kinetics is also observed in neat 1-MN; here the formation of the 1-MN triplet can be described with one time constant of $\tau \sim 1.8$ ps (see the behavior of the

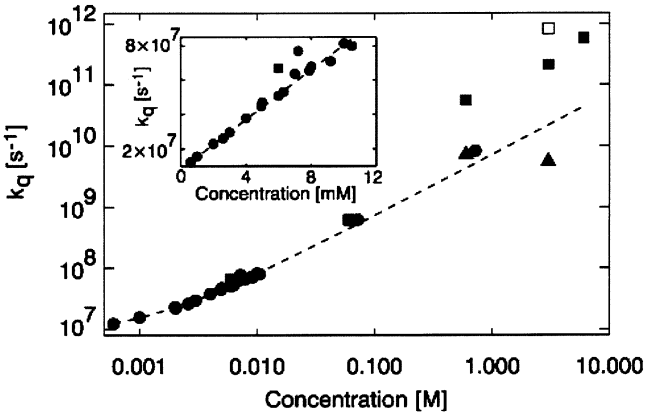

Figure 7. Dynamic quenching rate constant in dependence on the 1-MN concentration. The large (log−log) plot includes nanosecond (●) and femtosecond data (▲ for the slowest component, ■ and □ for the faster components). The insert focuses on the nanosecond experiments.

rise of the 1-MN triplet absorption in the upper part of Figure 6, curve e). In this static limit, the xanthone molecule is surrounded by quenchers at the instant of photoexcitation and no diffusional motion is required to induce the quenching process. The triplet quenching in this limit is faster than the slower component (12 ps) in the formation of the triplet absorption of xanthone in neat ethanol.

Quenching Kinetics: Intermediate Concentration Range and the 3.0 M Anomaly. Of course there is a smooth transition between the dynamic and the static regimes. A concentration of 0.6 M 1-MN nicely marks this interim domain where both regimes leave their kinetic imprint. The slow component of 120 ps obeys the prediction of eq 2, but faster components of 15 ps and even 2 ps for the rise of the 1-MN triplet absorption represent a static contribution to the quenching. Such complex kinetics is frequently observed for bimolecular photoprocesses provided that one of the reaction partners is present in high concentrations. Often these studies addressed the quenching of excited singlet states (for a review which includes theoretical description see ref 22), but an identical behavior should prevail in triplet quenching.

The 3.0 M experiment deviates from the smooth trend from a dynamic to a static behavior. On short time scales, the 2 ps component dominates the quenching kinetics. Thus, static quenching is the exclusive mechanism in that time domain. Quite surprisingly, in addition to this picosecond process the decay kinetics of the xanthone triplet contains a component with a time constant of ∼3 ns. This time is longer than the 120 ps observed for the dynamic quenching in the 0.6 M experiment. At present, a final explanation of this anomaly cannot be given. It might have its origin in the mixing thermodynamics of 1-MN and ethanol in combination with preferential solvation. Aromatic hydrocarbons (like 1-MN) and alcohols are known to have positive mixing enthalpies ΔH_m,[23] and this endothermicity usually peaks for a molar fraction of 0.5 of one of the constituents.[24] A concentration of 3.0 M 1-MN in ethanol corresponds to a molar fraction of 0.3. Typical peak values for ΔH_m are 1 kJ/mol,[24] which is close to the term of the entropy gain $T\Delta S_m$ which equals ∼1.6 kJ/mol[25] for ideal solutions. Therefore, the free energy change of mixing ΔG_m will be close to zero and these solutions are at the edge of separation. It is to be expected that such a solution microscopically consists of clusters where 1-MN is enriched and others where ethanol is enriched. The xanthone molecules could then be partitioned between these clusters. The rather polar xanthone molecule might dominately be solvated by ethanol. Examples for such a preferential solvation are abundant in the literature (see e.g. ref 26 and references therein). With these findings, one could derive a model for the 3.0 M anomaly. A fraction of the xanthone molecules are situated in ethanol clusters. Their triplet states are quenched slowly as the 1-MN molecules have to diffuse into these clusters. The other fraction is surrounded by 1-MN molecules, and rapid static quenching is possible. This is of course only a hypothesis, and its validation requires further experiments. For the purpose of this paper, it can be set aside since on the time scale of interest here (piocoseconds) the 3.0 M experiment is in line with those at other concentrations, particularly with that in neat 1-MN.

Quenching Mechanism: Energy Transfer versus Electron Transfer. In neat 1-MN, the formation of a 1-MN triplet with a time constant of 1.8 ps is faster than the slower component of the rise of the triplet absorption of xanthone in ethanol (12 ps). An interpretation of this surprising finding requires a discussion of the quenching mechanism. Two processes may contribute to the ultrafast quenching: triplet energy transfer and electron transfer generating a radical pair consisting of a 1-MN cation and a xanthone anion. Based on photocurrent measurements, Högemann and Vauthey excluded an electron-transfer quenching of triplet xanthone by 1-MN.[16] For naphthalenes with a less positive oxidation potential, an electron transfer is found to occur. This behavior is explained by the energetics of the process. While the gain of free energy ΔG is essentially zero for the electron transfer between triplet xanthone and 1-MN, it is negative for naphthalenes with a less positive oxidation potential, and electron transfer is feasible. However, for an electron transfer starting from an excited singlet state of xanthone the free energy released during electron transfer is higher than for the triplet electron transfer. The energy of a radical pair is virtually independent of its spin state,[27] and the energy of the initial states is larger by the singlet triplet splitting of xanthone (∼0.3 eV[19]). Therefore, starting from singlet excited xanthone electron transfer is exergonic by ∼0.3 eV and fast electron transfer cannot be excluded. In the experiments presented in ref 16, due to the low (0.1 M) quencher concentrations such a singlet electron transfer could not occur since the intersystem crossing is finished before donor and acceptor meet. For the experiments in neat 1-MN presented here, one could imagine that electron transfer offers an additional decay channel for the excited singlet state.

Several observations allow quenching by electron transfer to be excluded. First, within the accuracy of transient absorption experiments the absorbance of triplet 1-MN after termination of the quenching is identical for different 1-MN concentrations. In other words, the yield of triplet 1-MN shows no dependence on the quencher concentration. Since electron transfer would constitute a competing quenching mechanism, one would expect a reduction of the triplet yield for high quencher concentrations. Second, in the experiments on xanthone in neat 1-MN no spectral signature of the xanthone anion nor of the 1-MN cation is detected. The respective signatures should be observed in a spectral range of 550−720 nm.[16] After the ultrafast decay of the xanthone triplet spectrum within 1 ps, no longer lived signatures can be seen in this region. Thus the radical pair, if formed, has to be generated and has to recombine within less than 1 ps. Considering the highly different free energies which are released in both processes (−0.3 eV for the formation of the singlet radical pair and −3.18 eV[16] for its recombination), simple calculations based on the Marcus theory exclude ultrafast kinetics for both processes. Therefore, for the following it seems justified to take only energy transfer mechanisms into account.

Quenching Mechanism: Branched versus Sequential Kinetics. The absence of the 12 ps time constant in neat 1-MN can only be understood if all xanthone molecules undergo ISC with a time constant of 1.5 ps. Thus, the data are not compatible with a branched mechanism as described by Figure 2a. In that mechanism, the slow component would originate from the ISC between the $^1n\pi^*$ and the $^3\pi\pi^*$ state. A quenching of the $^1n\pi^*$ state by singlet−singlet energy transfer between excited xanthone and 1-MN is not feasible since the excited singlet state of 1-MN lies energetically well above that of xanthone.[21] A singlet triplet energy transfer though energetically possible is spin-forbidden and will not occur between different molecules with such a short time constant. Therefore, the slow component of the triplet formation cannot be assigned to the depletion of the $^1n\pi^*$ and the branched mechanism must be excluded. In the sequential mechanism, the only deactivation channel of the primarily excited $^1\pi\pi^*$ state is the fast ISC process to the $^3n\pi^*$ state. That state then decays via slower (12 ps) IC to the $^3\pi\pi^*$ state. Already after the first transition the complete population resides in a state of triplet multiplicity. This state *can* be quenched via triplet−triplet energy transfer, and the disappearance of the longer lived component of the xanthone triplet rise in the quenching experiments is naturally explained.

What seems in conflict with this mechanism is the finding reported in ref 8 by Cavaleri et al. that a biphasic rise of the triplet absorption is found irrespective of the solvent polarity. With changing polarity, the energy gap between the $^3n\pi^*$ state and the $^3\pi\pi^*$ state is known to vary.[19] Cavaleri et al. assume, in line with ref 19, that even an inversion occurs; that is, in polar solvents the $^3\pi\pi^*$ state is lowest in energy whereas it is the $^3n\pi^*$ state in nonpolar surroundings. Since El-Sayed's rules require that an ISC process starting in the $^1\pi\pi^*$ state will end up in a $^3n\pi^*$ state, in a nonpolar solvent the *lowest* triplet state would be directly populated. In our model which claims that the $^1\pi\pi^* \rightarrow {}^1n\pi^*$ IC is slow, this would imply a single-exponential ISC behavior in nonpolar solvents, in contradiction to the findings of Cavaleri et al. However, the inversion of the triplet states has been questioned by Connors et al.[28,29] They performed temperature-dependent phosphorescence experiments indicating that the energy gap between the triplet states is very small in nonpolar solvents but that the $^3\pi\pi^*$ state remains the state of lowest energy. The energy gap is smaller than kT at room temperature, and the $^3\pi\pi^*$ state can "behave" like a $^3n\pi^*$ state via thermal activation. Thus, the energetic ordering $^1\pi\pi^*$, $^3n\pi^*$, and $^3\pi\pi^*$ on which our sequential model depends seems to hold irrespective of the solvent polarity.

In the sequential mechanism proposed here, the ISC process from the $^1\pi\pi^*$ state to the $^3n\pi^*$ state is faster than the following IC process within the triplet manifold. This might be somewhat surprising. Yet, for El-Sayed allowed ISC processes the electronic couplings mediating the ISC transitions can be of the same order of magnitude as those of IC processes. For xanthone, this is supported by recent high-resolution spectra.[30] Still, one might argue that the IC process should be faster because of the energy gap law.[5] The energy gap between the triplet states is smaller than the pertinent separation of the $^1\pi\pi^*$ state and the triplet states. As the energetic separations are rather small, a few 1000 cm^{-1} for the ISC and a few 100 cm^{-1} for the IC process, a breakdown of the energy gap law is at least not unlikely, since the energies released in the transitions approach the value of typical vibrational quanta. A thorough analysis would require a quantum chemical treatment not only of the Franck−Condon factors (replacing the energy gap term) but also of the respective coupling elements. Here, we just stress that our experimental kinetic data point to an ISC process that is faster than IC.

4.2. Ultrafast Quenching Dynamics. The experiments on the triplet quenching at different 1-MN concentrations can also be used to obtain information on the quenching process itself. At low 1-MN concentrations, see Figures 5 and 6, exponential kinetics with a linear concentration dependence of the quenching rates is obtained. This is expected from the Smoluchowski−Stokes−Einstein treatment (see eq 2). At higher quencher concentrations, deviations from the single-exponential behavior result. At the highest concentrations, a single-exponential rise of the 1-MN triplet absorption is found with the time constant of the xanthone triplet formation (see above). This single exponentiality and the low transient concentration of the precursor state (see lower part Figure 6, curve e), the xanthone triplet, indicate that the transition rate $k^{3X\rightarrow 3(1\text{-MN})} = 1/\tau^{3X\rightarrow 3(1\text{-MN})}$ from the triplet of xanthone to 1-MN is considerably faster ($\tau < 1$ ps) than the formation time (1.5 ps) of the xanthone triplet itself. From the experiments with neat 1-MN as a solvent, we cannot decide whether the fast quenching rate is due to single, well-placed quenching molecules or due to the large number of 1-MN molecules in contact with the triplet donor.

A distinction between the two scenarios should be possible based on the quenching experiments at lower 1-MN concentrations. Lowering this concentration decreases the average number of acceptor molecules surrounding the xanthone donor. If the rate constant of the static quenching were dependent on that number, one would expect a decrease of the rate constant of the fastest component. Let us consider the experiments with a 1-MN concentration of 0.6 M. The rise of the 1-MN triplet absorption, which is directly related to the energy transfer, can be described by three time constants: 2 ps (relative contribution of 30%), 15 ps (40%), and 120 ps (30%). The process associated with the longest time constant obeys eq 2 and is therefore assigned to dynamic quenching. The 15 ps component is assigned to the transition regime between static and dynamic quenching. The 2 ps contribution finally is due to purely static quenching. This time constant is identical to the one observed for neat 1-MN, that is, with a quencher concentration 10 times higher. In other words, only the amplitude of the static quenching but not its rate constant decreases with concentration. Thus, the rate constant for the static quenching does not scale with the number of acceptors in close contact. It seems to be sufficient to have a single 1-MN in contact with triplet excited xanthone for energy transfer within ≤ 1 ps to occur. Such a behavior is not covered by the usual treatments of bimolecular quenching such as the Collins−Kimball approach[31] and the more sophisticated models mentioned in ref 22.

5. Conclusion

The investigation of transient emission and absorption in a wide range of wavelengths on xanthone and xanthone/1-methylnaphthalene solutions yielded important new information on the ISC in xanthone and on triplet quenching. It was shown that triplet formation after optical excitation of xanthone is an ultrafast process. The reaction is sequential, proceeding from the $^1\pi\pi^*$ to the $^3n\pi^*$ state within 1.5 ps and followed by a slower (12 ps) internal conversion in the triplet manifold to the $^3\pi\pi^*$ state. 1-Methyl-naphthalene acts as an efficient and ultrafast quencher for the xanthone triplet state. Quenching occurs on the 1 ps time scale. The experiments show that the system xanthone/1-methyl-naphthalene can be used for the study of very fast structural dynamics of peptides even on the picosecond time scale.

Acknowledgment. Dedicated to Professor Ulrich E. Steiner on the occasion of his 60th birthday.

References and Notes

(1) Bieri, O.; Wirz, J.; Hellrung, B.; Schutkowski, M.; Drewello M.; Kiefhaber, T. *Proc. Natl. Acad. Sci. U.S.A.* **1999**, *96*, 9597.

(2) Krieger, F.; Fierz, B.; Bieri, O.; Drewello, M.; Kiefhaber, T. *J. Mol. Biol.* **2003**, *332*, 265.

(3) Krieger, F.; Fierz, B.; Axthelm, F.; Joder, K.; Meyer, D.; Kiefhaber, T. *Chem. Phys.*, in press.

(4) Scaiano, J. C. *J. Am. Chem. Soc.* **1980**, *102*, 7747.

(5) *Modern Molecular Photochemistry*; Turro, N., Ed.; Benjamin/Cummings: Menlo Park, CA, 1978.

(6) Damschen, D. E.; Merritt, C. D.; Perry, D. L.; Scott, G. W.; Talley, L. D. *J. Phys. Chem.* **1978**, *82*, 2268.

(7) Greene, B. I.; Hochstrasser, R. M.; Weisman, R. B. *J. Chem. Phys.* **1979**, *70*, 1247.

(8) Cavaleri, J.; Prater, K.; Bowman, R. *Chem. Phys. Lett.* **1996**, *259*, 495.

(9) El-Sayed, M. *J. Chem. Phys.* **1963**, *38*, 2834.

(10) Schmidt, B.; Laimgruber, S.; Zinth, W.; Gilch, P. *Appl. Phys. B* **2003**, *76*, 809.

(11) Satzger, H.; Spörlein, S.; Root, C.; Wachtveitl, J.; Zinth, W.; Gilch, P. *Chem. Phys. Lett.* **2003**, *372*, 216.

(12) Seel, M.; Wildermuth, E.; Zinth, W. *Meas. Sci. Technol.* **1997**, *8*, 449.

(13) Strickler, S.; Berg, R. *J. Chem. Phys.* **1962**, *37*, 814.

(14) Ley, C.; Morlet-Savary, F.; Fouassier, J. P.; Jacques, P. *J. Photochem. Photobiol., A* **2000**, *137*, 87.

(15) Hochstrasser, R. A., Jr.; Lutz, H.; Scott, G. W. *J. Chem. Phys.* **1974**, *61*, 2500.

(16) Högemann, C.; Vauthey, E. *J. Phys. Chem. A* **1998**, *102*, 10051.

(17) Melhuish, W. *J. Chem. Phys.* **1969**, *50*, 2779.

(18) Wang, X.; Kofron, W.; Kong, S.; Rajesh, C.; Modarelli, D.; Lim, E. *J. Phys. Chem. A* **2000**, *104*, 1461.

(19) Pownall, H. J.; Huber, J. R. *J. Am. Chem. Soc.* **1971**, *93*, 6249.

(20) Morlet-Savary, F.; Ley, C.; Jacques, P.; Wieder, F.; Fouassier, J. P. *J. Photochem. Photobiol., A* **1999**, *126*, 7.

(21) *Handbook of Photochemistry*; Murov, S. L., Carmichael, I., Hug, G. L., Eds.; Marcel Dekker: New York, 1993.

(22) Sikorski, M.; Krystkowiak, E.; Steer, R. *J. Photochem. Photobiol., A* **1998**, *117*, 1.

(23) Ott, J.; Sipowska, J. *J. Chem. Eng. Data* **1996**, *41*, 987.

(24) Lien, P.; Lin, H.; Lee, M. *Fluid Phase Equilib.* **2004**, *215*, 187.

(25) Atkins, P.; de Paula, J. *Physical Chemistry*, 7th ed.; Oxford University Press: Oxford, 2002.

(26) Jozefowicz, M.; Heldt, J. *Chem. Phys.* **2003**, *294*, 105.

(27) Steiner, U. E.; Ulrich, T. *Chem. Rev.* **1989**, *89*, 51.

(28) Connors, R. E.; Christian, W. R. *J. Phys. Chem.* **1982**, *86*, 1524.

(29) Connors, R. E.; Sweeney, R. J.; Cerio, F. *J. Phys. Chem.* **1987**, *91*, 819.

(30) Ohshima, Y.; Fujii, T.; Fujita, T.; Inaba, D.; Baba, M. *J. Phys. Chem. A* **2003**, *107*, 8851.

(31) Collins, F. C.; Kimball, G. E. *J. Colloid. Sci.* **1949**, *4*, 425.

(32) The time constant determined by transient absorption is 1.3 ps, and by fluorescence spectroscopy 1.5 ps. In the following we will refer to both as the 1.5 ps component.